



저작자표시 2.0 대한민국

이용자는 아래의 조건을 따르는 경우에 한하여 자유롭게

- 이 저작물을 복제, 배포, 전송, 전시, 공연 및 방송할 수 있습니다.
- 이차적 저작물을 작성할 수 있습니다.
- 이 저작물을 영리 목적으로 이용할 수 있습니다.

다음과 같은 조건을 따라야 합니다:



저작자표시. 귀하는 원저작자를 표시하여야 합니다.

- 귀하는, 이 저작물의 재이용이나 배포의 경우, 이 저작물에 적용된 이용허락조건을 명확하게 나타내어야 합니다.
- 저작권자로부터 별도의 허가를 받으면 이러한 조건들은 적용되지 않습니다.

저작권법에 따른 이용자의 권리는 위의 내용에 의하여 영향을 받지 않습니다.

이것은 [이용허락규약\(Legal Code\)](#)을 이해하기 쉽게 요약한 것입니다.

[Disclaimer](#) 

Effect of lactoferrin-anchored tannylated
mesoporous silica nanomaterials on spinal
fusion in a rat model

Sung Hyun Noh

Department of Medicine

The Graduate School, Yonsei University

Effect of lactoferrin-anchored tannylated mesoporous silica nanomaterials on spinal fusion in a rat model

Directed by Professor Keung Nyun Kim

The Doctoral Dissertation
submitted to the Department of Medicine,
the Graduate School of Yonsei University
in partial fulfillment of the requirements for the degree of
Doctor of Philosophy in Medical Science

Sung Hyun Noh

December 2023

<Signature page>

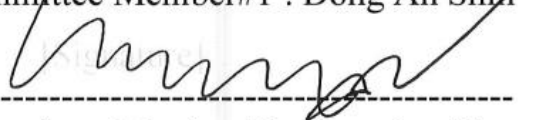
This certifies that the Doctoral Dissertation of
Sung Hyun Noh is approved.

[Signature]

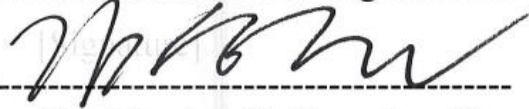
Thesis Supervisor : Keung Nyun Kim



Thesis Committee Member#1 : Dong Ah Shin



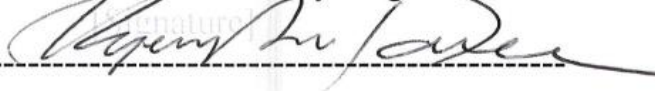
Thesis Committee Member#2 : Sung Jun Kim



Thesis Committee Member#3 : Sung Eun Kim



Thesis Committee Member#4 : Kyeong Soon Park



The Graduate School
Yonsei University

December 2023

ACKNOWLEDGEMENTS

While pursuing my Doctoral Dissertation, many people helped me successfully complete my study. I would like to express my gratitude through this article.

I would like to thank Professor Keung Nyun Kim for his help and guidance both materially and spiritually until the research was completed. I was able to successfully complete the research thanks to his encouragement and generous advice until the end of the experiment.

I would like to thank Professor Sung Eun Kim for giving me an idea for a research topic and pointing me in the right direction. Even though he was busy, he taught me in a thorough and thorough manner, so I learned a lot. As he said, I will always be grateful and do my best to achieve it with a loving heart.

It is God who brought me to this status. Thank you for God. I would also like to thank my wife, Professor Mi Hyun Song, and my lovely daughters Eun-Woo and Eun-Jae, who always support me.

I will remember that this study was completed with insufficient grace and help, and I will humbly work harder to become a student my teachers can be proud of.

<TABLE OF CONTENTS>

ABSTRACT.....	iii
I. INTRODUCTION	1
II. MATERIALS AND METHODS	3
1. Animals	3
2. Materials	3
3. Experimental design and surgical procedure	4
4. Manual palpation	6
5. Micro CT	6
6. Histologic evaluation	7
7. Bone turnover marker.....	7
8. Quantification of osteo-differentiation specific genes	8
9. Statistical analysis.....	8
III. RESULTS	8
1. Manual palpation	9
2. Micro CT	10
3. Histologic results.....	12
4. Bone turnover marker.....	14
5. Quantification of osteo-differentiation specific genes	14
IV. DISCUSSION	15
V. CONCLUSION	18
REFERENCES	19
ABSTRACT (IN KOREAN)	24
PUBLICATION LIST	26

LIST OF FIGURES

Figure 1. Experimental process	5
Figure 2. The representative cases of micro-CT.....	11
Figure 3. Histologic analysis of H&E	12
Figure 4. Histologic analysis of osteocalcin	13
Figure 5. Serum osteocalcin by ELISA	14
Figure 6. The mRNA expression of Osteocalcin and Osteopontin..	15

LIST OF TABLES

Table 1. Qualitative fusion assessment by manual palpation at 8 weeks after fusion	9
Table 2. Quantitative results of micro-CT findings at 8 weeks after fusion	10
Table 3. Semiquantitative histological evaluation in the frequency of blood vessels	13

ABSTRACT

Effect of lactoferrin-anchored tannylated mesoporous silica nanomaterials on spinal fusion in a rat model

Sung Hyun Noh

*Department of Medicine
The Graduate School, Yonsei University*

(Directed by Professor Keung Nyun Kim)

Lactoferrin (LF) is a potent antiviral, anti-inflammatory, and antibacterial agent found in cow and human colostrum. Additionally, it acts as an osteogenic growth factor. This study aimed to investigate whether LF functions as a bone fusion material in a rat model. We created LF-anchored tannylated mesoporous silica nanomaterials (TA-MSN-LF) and measured the effects of low (1 μg) and high (100 μg) TA-MSN-LF concentrations in a spinal fusion animal model. Rats were assigned to four groups: defect, MSN, TA-MSN-LF-Low (1 $\mu\text{g}/\text{mL}$), and TA-MSN-LF-High (100 $\mu\text{g}/\text{mL}$). A greater amount of radiological fusion was identified in the TA-MSN-LF groups than in the other groups eight weeks after surgery. Hematoxylin and eosin staining revealed newly induced bone fusion in the TA-MSN-LF groups. Osteocalcin, a marker of bone formation, was detected through immunohistochemistry, and its intensity was induced in the TA-MSN-LF groups. Moreover, new vessels were formed in the TA-MSN-LF-High group. The serum osteocalcin level and mRNA expression of osteocalcin and osteopontin were increased in the TA-MSN-LF groups. Furthermore, TA-MSN-LF showed effective bone fusion and angiogenesis in rats. These findings suggest that TA-MSN-LF is a potent material for spinal bone fusion.

Key words: lactoferrin, bone fusion, rat, spine, nanoparticles

Effect of lactoferrin-anchored tannylated mesoporous silica nanomaterials on spinal fusion in a rat model

Sung Hyun Noh

*Department of Medicine
The Graduate School, Yonsei University*

(Directed by Professor Keung Nyun Kim)

I. INTRODUCTION

Spinal fusion is an increasingly common procedure used to treat various pathologies arising from trauma, degenerative diseases, infections, and tumors.¹ However, pseudarthrosis can occur because of a bone fusion failure, resulting in pain, instability, and disability.² Failure of bone bridging increases the risk of device failure, with sedimentation or screw loosening observed.³ Pseudarthrosis rates range from 5% to 34%.⁴ Successful bone fusion after spinal fusion is challenging, particularly in elderly patients with osteoporosis, owing to low bone strength and poor bone quality. Several treatment modalities have been explored to prevent fusion failure or pseudarthrosis over the past decade, with research focusing on the identification of new substances that aid fusion.

Employing autograft iliac crest bone is the clinical "gold standard" in fusion procedures. However, these autografts have several disadvantages. Collecting a consistent volume of the iliac crest bone may be difficult. In addition, the harvesting procedure can be painful and may be associated with hematomas, infections, fractures at the donor location, and prolonged surgical time. Furthermore, there are limitations in the use of bone autografts in patients with osteoporosis or metabolic diseases.

Spine surgeons have used various other methods outside autologous bone graft material, including allogeneic bone graft materials (e.g., demineralized bone allograft), synthetic

bone graft materials (e.g., tricalcium phosphate, hydroxyapatite, bioglass), and bone morphogenetic protein-2 (BMP2), to achieve bone fusion.⁵ BMP2 was approved for clinical use in 2002 and is currently used for spinal fusion. Although this protein is effective in osteogenic differentiation and osteogenesis, delivery of BMP2 alone is not effective in supporting osteogenesis due to its short half-life. BMP2 diffuses rapidly throughout bodily fluids and is cleared rapidly.⁶ Therefore, higher than physiological doses of BMP2 have been clinically used to promote bone formation. However, high doses of BMP2 are associated with serious complications such as soft tissue inflammation and heterotopic ossification.⁷

Lactoferrin (LF), an 80 kDa non-heme iron-binding protein produced primarily by exocrine epithelial cells and expressed in most tissues, plays an important role in the innate immune system of mammals.⁸ LF is a potent antiviral, anti-inflammatory, and antibacterial agent found in cow and human colostrum.⁹ Moreover, LF acts as an osteogenic growth factor. Treatment with LF not only increases osteoblast proliferation but also promotes osteoblast differentiation.⁸ Previous studies have examined the oral administration and local injection of LF.¹⁰⁻¹² Yanagisawa et al.¹⁰ found that oral administration of LF suppressed the progression of rheumatoid arthritis in a mouse model. Similarly, Guo et al.¹¹ revealed that oral administration of LF to ovariectomized rats preserved bone mass and improved bone microarchitecture. Furthermore, Cornish et al.¹² reported that local injection of LF over the hemicalvaria increases bone growth in adult male mice.

Tannic acid (TA), a hydrolysable natural polyphenol, is found in many plant-based foods and beverages such as green tea, coffee, red wine, hazelnuts, and walnuts.¹³ It can function as both an organic and inorganic specimen due to the existence of hydroxyl and galloyl groups.^{14,15} In addition, the electrostatic, hydrogen bonding, and hydrophobic interaction abilities of TA facilitate its direct interaction with several biomacromolecules, including DNA, gelatin, collagen, albumin, chitosan, thrombin, and enzymes.¹⁶ Mesoporous silica nanomaterials (MSNs) have recently attracted considerable attention for their potential biomedical applications, owing to their superior biocompatibility and biodegradability

compared to other inorganic nanomaterials.^{17,18} Moreover, their high surface area, large pore size, and easily modifiable surface have made MSNs a major research topic in bone tissue engineering.^{19,20} They have garnered attention as a promising drug nanovehicle that possesses not only a high drug loading ability, but also the ability to deliver time-dependent drug release.

A previous study examined LF-anchored tannylated MSNs (TA-MSN-LF).²¹ LF is a promising protein for osteogenic differentiation and tendon healing. However, without the assistance of a delivery medium, the effect of the protein drug was not as effective as expected because of its short half-life in the blood.²² Therefore, recent studies have focused on the use of MSN and TA, with the osteo-differentiation ability of TA-MSN-LF demonstrated *in vitro*.²¹ This study aimed to investigate whether TA-MSN-LF functions as a bone fusion material in a rat model of lumbar spinal fusion. To our knowledge, this is the first study to demonstrate the effectiveness of LF in an animal model of lumbar spinal fusion.

II. MATERIALS AND METHODS

2.1. Animals

All animal procedures were conducted according to the guidelines of the Laboratory Animal Center (Korea-2020-0059-C1). The experimental animals were housed in a specific pathogen-free facility and fed a standard diet. All animals used in this study were female Sprague-Dawley (SD) rats (weight, 100–180 g) aged 6–9 weeks.

2.2. Materials

MSNs (Sigma-Aldrich, St. Louis, MO, USA) were modified with TA (Sigma-Aldrich) to immobilize human LF (Sigma-Aldrich). First, 10 mg of MSN were added to a phosphate buffered saline (PBS) solution (pH, 7.4) containing dissolved TA (concentration, 50 µg/mL) and the mixture was gently shaken overnight at room temperature. MSNs containing TA

were then washed twice with distilled water (DW) and lyophilized for two days. The TA load on MSN was confirmed by analyzing the amount of residual TA in the PBS solution. Hereafter, the MSNs with TA are referred to as TA-MSNs.

To immobilize LF (concentration, 1 or 100 $\mu\text{g}/\text{mL}$) on the MSN surface, 10 $\mu\text{g}/\text{mL}$ TA-MSN and 1 or 100 $\mu\text{g}/\text{mL}$ LF were added to the PBS solution and then incubated for 24 h. Next, all samples were washed three times with DW at 3000 rpm and 4 $^{\circ}\text{C}$ for 10 min using a Smart R17 centrifuge (Hanil Science Industrial, Incheon, Korea). The samples were freeze-dried for two days.

The supernatant was collected after the immobilization of LF on TA-MSN and analyzed using the Pierce Bicinchoninic Acid (BCA) protein assay kit (Thermo Fisher Scientific, Rockford, IL, USA) according to the manufacturer's protocol to assess the LF load. The 1 $\mu\text{g}/\text{mL}$ LF and 100 $\mu\text{g}/\text{mL}$ LF anchor-type TA-MSNs are hereafter referred to as TA-MSN-LF low and TA-MSN-LF high, respectively. Three milligrams was used in the experiment, and the real LF dose was calculated when 3 mg of TA-MSN-LF was added, which was 0.03 $\mu\text{g}/\text{rat}$ (1 $\mu\text{g}/\text{mL}$ TA-MSN-LF) and 2.75 $\mu\text{g}/\text{rat}$ (100 $\mu\text{g}/\text{mL}$ TA-MSN-LF). The use of TA-MSN-LF low (1 $\mu\text{g}/\text{mL}$) and TA-MSN-LF high (100 $\mu\text{g}/\text{mL}$) in our study was based on previous studies.²⁷⁻²⁹ Chang et al.²⁷ evaluated the osteo-differentiation of adipose-derived stem cells at varying LF doses (10 $\mu\text{g}/\text{mL}$, 20 $\mu\text{g}/\text{mL}$, 50 $\mu\text{g}/\text{mL}$, 100 $\mu\text{g}/\text{mL}$, and 500 $\mu\text{g}/\text{mL}$) and concluded that 100 $\mu\text{g}/\text{mL}$ was the most effective dose. Li et al.²⁸ studied LF doses of 1 μg , 10 μg , 100 μg , and 1000 μg , whereas Zhang et al.²⁹ studied LF doses of 1 μg , 10 μg , and 100 μg . Therefore, we compared 1 $\mu\text{g}/\text{mL}$ and 100 $\mu\text{g}/\text{mL}$ doses in the present study.

2.3. Experimental design and surgical procedure

A single-level bilateral lumbar posterolateral fusion was performed, and thirty host rats were divided into four experimental groups: [A] LF (100 μg) anchor-type TA-MSN (n = 8), [B] LF (1 μg) anchor-type TA-MSN (n = 8), [C] MSN (n = 8), and [D] Defect (n = 6). The rats were anesthetized with a zoletil-xylazine solution (20 mg/kg zoletil and 10 mg/kg

xylazine) and the surgical site was shaved. The vertebral levels from L4 to L5 were identified by palpation and anatomical landmarks. A dorsal midline skin incision was made at the center of the L4-L5 spinous processes, and the edges of the skin were retracted using a self-holding aspirator. An intermuscular plane was established between the multifidus and longissimus muscles, thereby exposing the transverse process from L4 to L5. Decortication of the transverse processes and external segments/intervertebral joints was performed using an electric bar. After decorticating the transverse processes on both sides of L4 and L5, 3 mg of each material was implanted on each side of the fusion bed space (L4-L5). Then, cefazolin (100 mg/kg) was injected after suturing the muscle and skin layer-by-layer. The rats were euthanized eight weeks after the experiment. Figure 1 illustrates the surgical process.

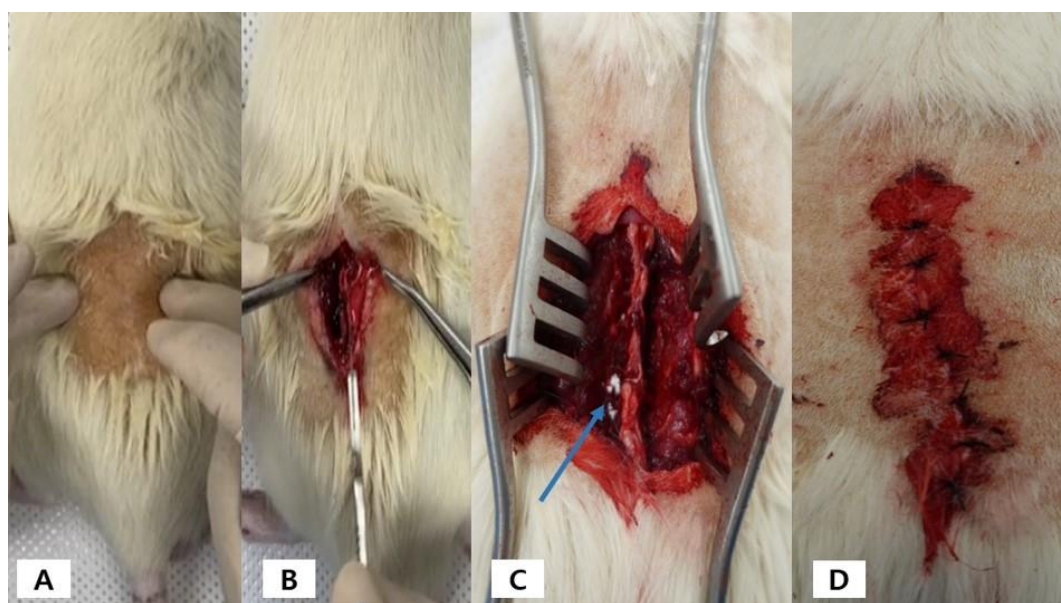


Figure 1. (A) After anesthetizing the rat, the hair of the experimental area is shaved. (B) The skin is incised, and the muscles are dissected. (C) Materials were placed on the decorated area. (Blue arrow) (D) The fascia and skin were sutured.

2.4. *Manual palpation*

The lumbar spine specimens were carefully collected eight weeks after the fusion surgery, and the soft tissue around the specimens was carefully removed. The qualitative degree of fusion, degree of hardness, and amount of bridged bone were investigated to evaluate the degree of fusion. Flexion, extension, side flexion, and torsion forces were applied, and the qualitative fusion grade was measured as follows: Grade (1), a nonunion state in which the range of motion of the index part presented as that of a normal lumbar spine; Grade (2), a fused state in which the range of motion of the index part was reduced but presented some flexibility; Grade (3), a state in which the range of motion of the index part was absent. the motion in the stationary state was smooth, and the hardness was similar to that of a hard bone.

The degree of hardness of the fused portion was examined using direct finger pressure and classified according to the following subjective judgment: Grade (1), no or minimal hardness; Grade (2), hard but not satisfying hard bone; and Grade (3), hard bone-like absolute hardness. The volume of the bridging bone between the transverse processes was evaluated using direct visual inspection and finger palpation and was classified as follows: Grade (1), no or minimal volume of bridging bone; Grade (2), flat bone-like apparent volume; and Grade (3), flower-like excess volume compared with flat bone. Passive qualitative fusion scores were rated from 0 to 9 according to the sum of all grades obtained by manual palpation.

2.5. *Micro-CT*

All samples were scanned using a high-resolution micro- computed tomography (CT) (SkyScan-1072, Skysan, Kontich, Belgium) running at 90 kV and 200 mA. SkyScan1173 control software (Ver 1.6, Bruker-CT, Billerica, MA, USA) was used under the following parameters for the measurement: tube voltage, 130 kVp; tube current, 60 μ A; aluminum filtration (Filter), 1 mm; exposure time, 500 ms; pixels, 2240 \times 2240; and pixel size, 35.00 μ m. Rotation angles of 0.3° and 180° were used to obtain 800 high-resolution images. An

image of 2240×2240 pixels was obtained using Nrecon (Ver 1.7.0.4, Bruker-CT) for cross-sectional reconstruction, and the cross-sectional image was aligned using Dataviewer (Version 1.5.1.2, Bruker-CT). The area was set using CTAn (Version 1.17.7.2, Bruker-CT) for data analysis, and the volume of the new bone area was analyzed by setting the threshold to 90–255 for the amount of bones present and bone parameters in the area. The bone union volume between the transverse processes was analyzed for quantitative fusion analysis. Scans of the newly formed bone were evaluated from the lower endplate of the lower spine to the upper endplate of the upper spine.

2.6. Histological evaluation

All spinal specimens were desalted in 10% formaldehyde solution for seven days and embedded in paraffin wax after radiographic examinations. Serial sections (thickness, 5 mm) through the largest defect diameter were stained with hematoxylin and eosin (H&E) to identify cellular responses indicative of osteogenesis. Serial sections (thickness, 5 mm) up to the maximum defect diameter were stained with H&E to evaluate cellular responses indicative of bone formation. Moreover, osteocalcin (OCN) expression was immunohistochemically analyzed. We measured OCN intensity and analyzed the quantity of blood vessels using a semi-quantitative histological evaluation. Blood vessel frequency was determined using the following scoring criteria: 1 = often; 2 = quite often; 3 = frequent; and 4 = very frequent.

2.7. Bone turnover marker

The quantitative osteogenic ability of each group to induce osteoblast activity was compared by evaluating serum OCN levels using an OCN ELISA kit (Novus, CA, USA). All standards and samples were analyzed using an iMark microplate reader (Bio-Rad, Hercules, CA, USA) at a wavelength of 450 nm.

2.8. Quantification of osteo-differentiation-specific genes

To further confirm the osteogenic capacity of MSNs with or without LF, the mRNA levels of osteogenic differentiation-specific genetic markers such as OCN and osteopontin (OPN) were examined using real-time polymerase chain reaction (PCR). Total RNA was purified using a TRIzol reagent, and cDNA was prepared from total RNA (1 μ g) using a PrimeScript™ 1st Strand cDNA synthesis kit (Takara Bio Inc., Otsu, Japan). PCR amplification and real-time PCR were performed using an ABI7300 Real-Time Thermal Cycler (Applied Biosystems, Foster City, CA, USA). *Ocn* and *Opn* were normalized to glyceraldehyde 3-phosphate dehydrogenase (GAPDH). All experiments were repeated three times at each time point. Expression levels were calculated using the $2^{-\Delta\Delta CT}$ method.

2.9. Statistical analysis

All statistical analyses were performed using IBM SPSS Statistics for Windows, Version 25.0 (IBM Corp., Armonk, NY, USA). Data are presented as the mean \pm standard deviation. Pearson's chi-square test, the nonparametric Wilcoxon rank-sum test, and centralized analysis of variance (ANOVA) were used depending on the nature of the parameters. Statistical significance was set to a p value < 0.05 .

III. RESULTS

Of the 33 rats, three died during surgery due to side effects of general anesthesia and 30 survived without complications. The behavior of the remaining animals showed no specific changes suggesting side effects of the chemicals or local complications such as nerve irritation. Finally, the lumbar fusion models used in the analyses were as follows: TA-MSN-LF high group, 8; TA-MSN-LF low group, 8; MSN group, 8; and Defect group, 6.

3.1. Manual palpation

Table 1 shows the qualitative fusion assessment by manual palpation at eight weeks after fusion. Qualitative parameters such as degree of fusion, degree of hardness, and volume of the bridged bone were significantly different between each group ($p < 0.001$). Additionally, the manual qualitative fusion scores were significantly different between each group ($p < 0.001$). All parameters derived from manual palpation showed better results in the TA-MSN-LF high group than in the other groups. These results demonstrate that promotion of bone fusion was superior in the TA-MSN-LF high group.

Table 1. Qualitative fusion assessment by manual palpation at 8 weeks after fusion

Characteristics	MSN group (n=8)	TA-MSN-LF low group (n=8)	TA-MSN-LF high group (n=8)	<i>P</i>
Fusion grade				
1	2	0	0	
2	6	3	1	
3	0	5	7	<0.001**
Degree of firmness				
1	5	0	0	
2	3	4	0	
3	0	4	8	<0.001**
Volume of bridging bone				
1	2	0	0	
2	5	2	0	
3	1	6	8	<0.001**

**P value < 0.01

3.2. Micro-CT

Table 2 shows the quantitative results of the micro-CT findings eight weeks after fusion. Micro-CT of the TA-MSN-LF high and low groups revealed new bone formation in the decortication area (Figure 2). Additionally, quantitative fusion bone volume and trabecular bone number were significantly different among the groups ($p < 0.05$). Bone volume and trabecular number in the TA-MSN-LF high group were higher than those in the other groups. However, there were no significant differences in trabecular bone thickness and separation among the four groups. These results demonstrate that promotion of bone fusion was superior in the TA-MSN-LF high group.

Table 2. Quantitative results of micro-CT findings at 8 weeks after fusion

	Defect group (n=6)	MSN group (n=8)	TA-MSN-LF low group (n=8)	TA-MSN-LF high group (n=8)	P
Bone Volume (mm ³)	84.761 ±8.507	99.697 ±14.234	114.701 ±15.703	121.335 ±4.204	<0.05*
Trabecular thickness (mm)	0.485±0.058	0.400±0.029	0.416±0.046	0.412±0.047	0.348
Trabecular number (1/mm)	0.152±0.022	0.179±0.030	0.211±0.015	0.212±0.020	<0.05*
Trabecular separation (mm)	4.500±0.343	4.409±0.246	4.277±0.238	4.307±0.425	0.637

*P value < 0.05

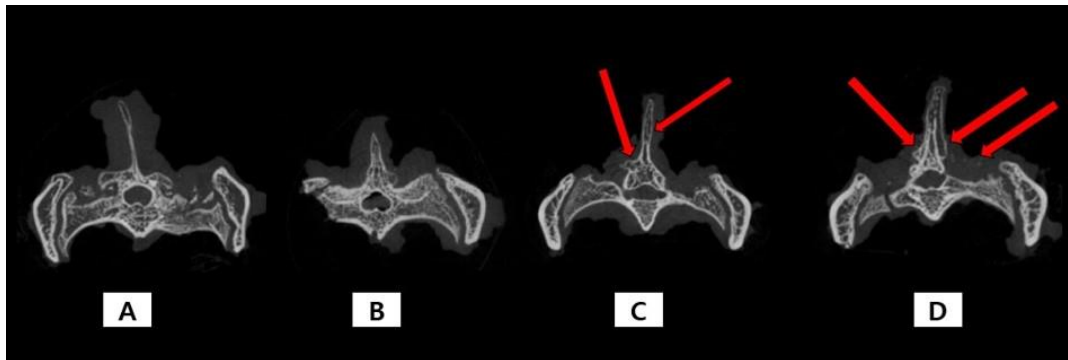


Figure 2. The representative cases of micro-CT. (A) Micro-CT of Defect group shows no new bone formation in decortication area. (B) Micro CT of MSN group shows no new bone formation in decortication area. (C) Micro-CT of TA-MSN-LF low group shows a few bone formation in decortication area. (red arrow) (D) Micro-CT of TA-MSN-LF high group shows a large bone formation in decortication area. (red arrow)

3.3. Histologic results

H&E and OCN staining were performed to evaluate new bone formation eight weeks after the procedure. As shown in Figure 3, new bone formation was observed in the TA-MSN-LF high and low groups. Figure 4A shows staining for OCN, a bone formation marker, in each group. Staining was best performed in the TA-MSN-LF high group. Figure 4B quantifies this and compares the OCN levels. The TA-MSN-LF high and low groups had significantly higher OCN intensity than the other groups ($p < 0.05$). The OCN intensity of the TA-MSN-LF-high group was significantly higher than that in the TA-MSN-LF low group ($p < 0.05$). Moreover, the blood vessel frequency in the TA-MSN-LF high group was significantly higher than that in the other groups ($p < 0.05$, Table 3). These histological results indicate that bone fusion and angiogenesis were most effective in the TA-MSN-LF high group.

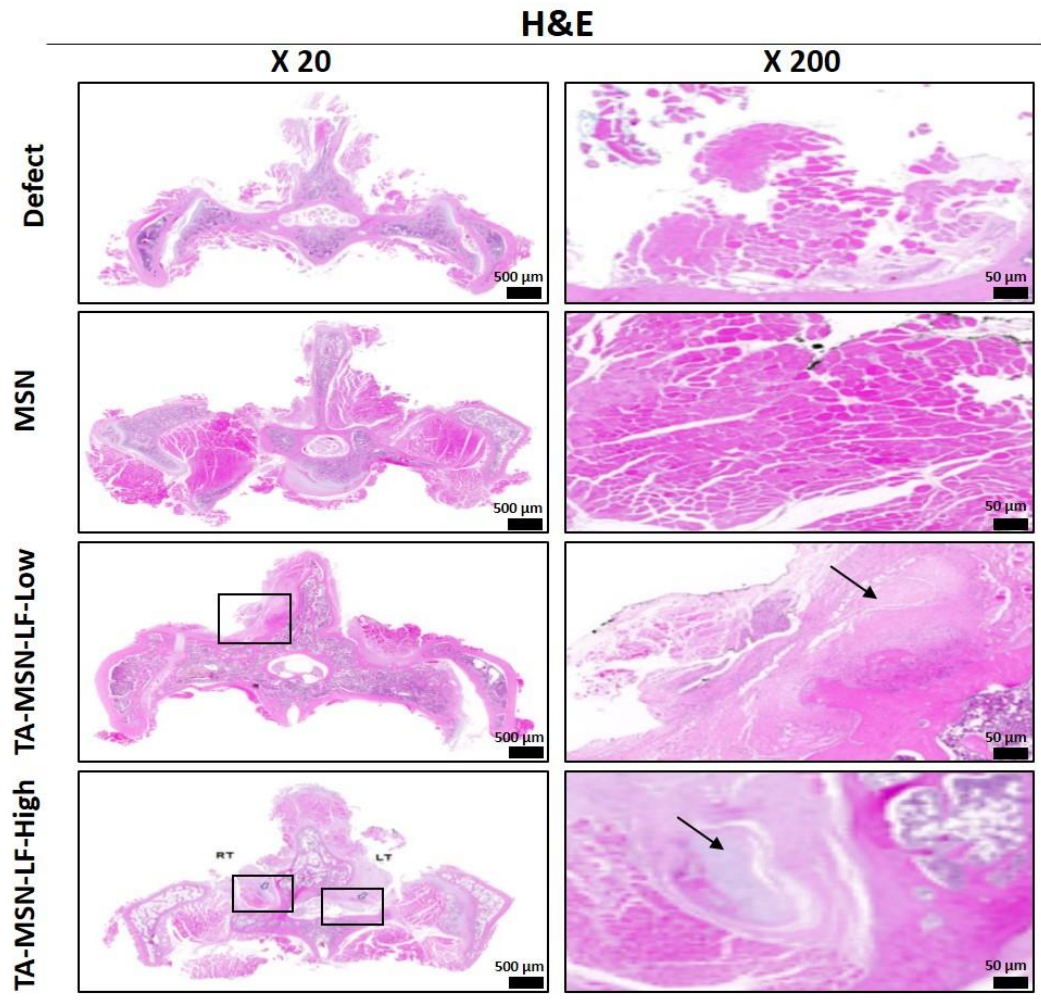


Figure 3. Histological analysis of Spinal Fusion Animal Model. Histological sections was stained with H&E and Boxes/black arrows indicate new bone formation. Scale bar = 500/50 μ m.

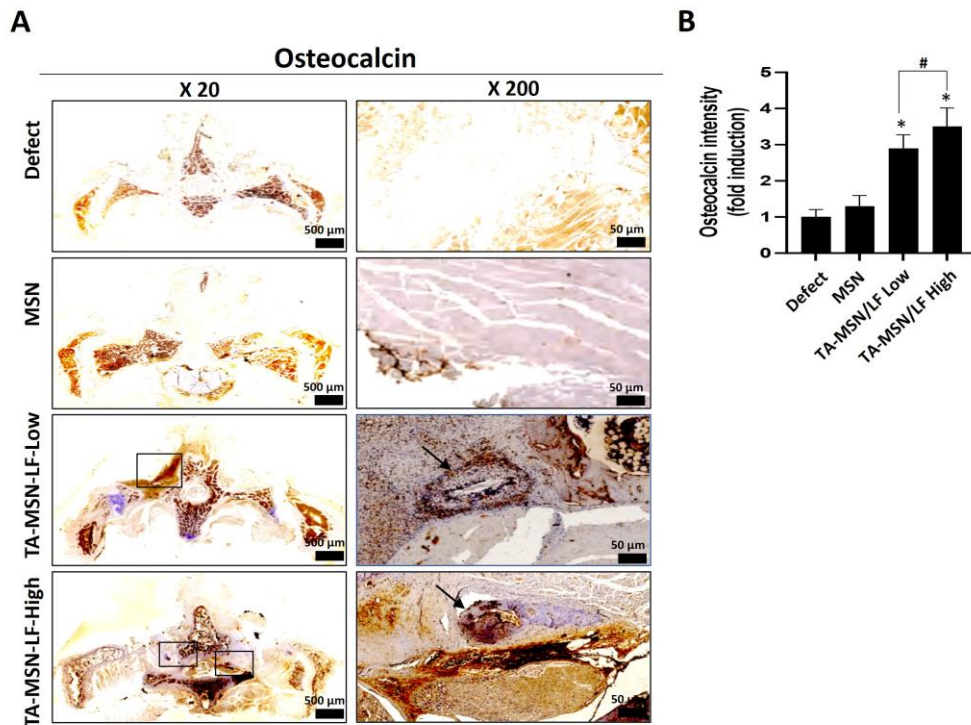


Figure 4. (A) Immunohistochemistry for osteocalcin. (B) Osteocalcin intensity. The data was expressed as mean \pm SEM in each bar graph. * $p < 0.05$ compared with Defect group. # $p < 0.05$ between two groups. The Boxes/black arrows indicate new bone formation. Scale bar = 500/50 μ m.

Table 3. Semiquantitative histological evaluation in the frequency of blood vessels

	Defect group (n=6)	MSN group (n=8)	TA-MSN-LF low group (n=8)	TA-MSN-LF high group (n=8)	<i>P</i>
Bone Volume (mm ³)	1.00 \pm 0.00	1.37 \pm 0.50	1.51 \pm 0.50	1.96 \pm 0.50	<0.05*

**P* value < 0.05

3.4. Bone turnover marker

The serum OCN concentration was significantly higher in the TA-MSN-LF high and low groups than that in the other groups ($p < 0.05$, Figure 5). Similarly, the serum OCN concentration of the TA-MSN-LF high group was significantly higher than that in the TA-MSN-LF low group ($p < 0.05$). These results show that bone fusion ability was the highest in the TA-MSN-LF high group.

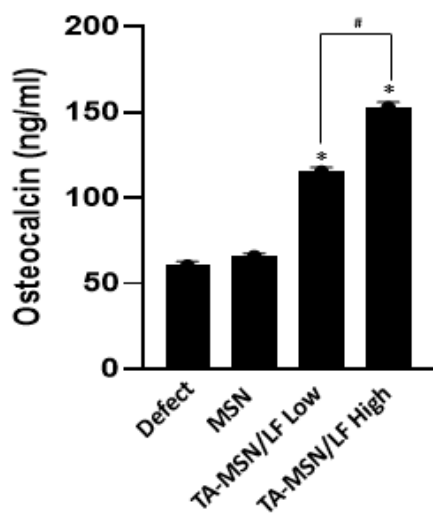


Figure 5. Serum osteocalcin by ELISA. The data was expressed as mean \pm SEM in each bar graph. * $p < 0.05$ compared with Defect group. # $p < 0.05$ between two groups.

3.5. Quantification of osteo-differentiation specific genes

The mRNA expression levels of OCN and OPN were significantly higher in the TA-MSN-LF high and low groups than in the other groups ($p < 0.05$, Figure 6). The mRNA expression levels of OCN and OPN in the TA-MSN-LF high group were significantly

higher than those in the TA-MSN-LF low group ($p < 0.05$). This suggests that high-dose TA-MSN-LF may promote and accelerate bone formation.

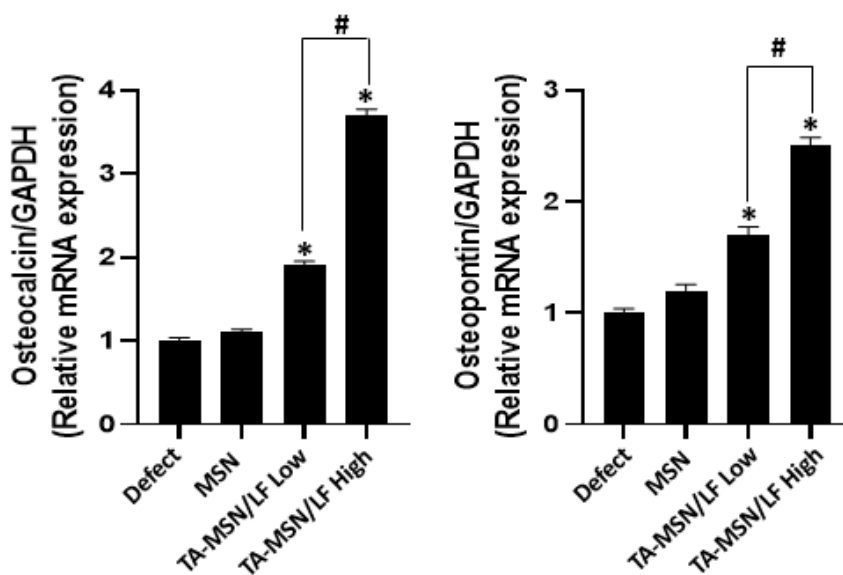


Figure 6. The mRNA expression of Osteocalcin and Osteopontin. The relative mRNA expression of each target was normalized to the GAPDH. Values are the means \pm SEM in each bar graph. * $p < 0.05$ compared with Defect group. # $p < 0.05$ between two groups.

IV. DISCUSSION

Although the development of new substances for bone-tissue regeneration remains challenging, numerous biomaterials have been proposed for this purpose. LF is an osteoinductive factor that can promote the osteogenic differentiation of various cells, such as osteoblasts, C2C12 cells, and adipose-derived stem cells.³⁰ In a previous study, we

developed a new type of TA-MSN-LF to release LF from nanoparticles over a long period and impart osteoconductive effects to the silica nanoparticles.²¹ In this study, this material was administered into rats to determine its effectiveness as a bone fusion material.

LF is a widely distributed glycoprotein in mammals; human tears contain approximately 1.13 g/L of LF and human colostrum contains >5 g/L.^{31,32} LF is a crucial anabolic bone growth factor and can function as an effector molecule for bone remodeling.³³ *In vitro* experiments have shown that local distribution of LF strongly increased the proliferation and differentiation of osteoblasts in mice and humans.^{34,35} Furthermore, the oral administration of LF not only improves bone formation and sclerosis in distraction osteogenic animal models but also improves bone mineral density and biomechanical strength in ovariectomized animal models.^{36,37}

LF was immobilized on an MSN surface coated with TA to construct the TA-MSN-LF model. TA is a representative molecule with a strong affinity for various proteins, such as proline-rich ones.³⁸ Each MSN group was observed through transmission electron microscopy, and dynamic light scattering was performed at 260–300 nm. We also used X-ray photoelectron spectroscopy to investigate the surface chemical composition of MSNs containing TA and/or LF. We subsequently compared this with the composition of pure MSNs. TA-MSN-LF exhibited a sustained release of LF for up to 28 days, demonstrating that TA-MSN-LF nanoparticles can achieve long-term delivery of LF. Park et al.³⁹ investigated whether local bone regeneration occurred in a rat calvarial defect model using LF and poloxamer gels, which were used as the LF carriers. However, LF was released for up to three days under these conditions. Thus, the LF/poloxamer material increased cell viability and was less likely to induce immune responses; however, the formulation failed to enhance bone regeneration *in vivo*. Conversely, the role of TA-MSN as a transmitter was significant in our study.

In this study, we evaluated whether TA-MSN-LF could induce the formation of bone tissue and spinal regeneration *in vivo* as an alternative to autologous bone. TA-MSN-LF significantly increased new bone tissue formation and vertebral bone regeneration eight

weeks after a spinal fusion procedure in a rat model. Additionally, the bone volume and trabecular number were significantly higher in the high-dose TA-MSN-LF group (<0.05). Guo et al.¹¹ analyzed the effects of oral LF on bone mass and microarchitecture in a rat model of osteoporosis. The LF dose was divided into three groups: 0.85 mg/kg body weight, 8.5 mg/kg body weight, and 85 mg/kg body weight. Micro-CT analysis revealed that bone volume was the highest in the 85 mg/kg body weight group. Koca et al.⁴⁰ investigated whether LF was beneficial for autograft healing in peri-implant bone in a rat model. The percentage of bone volume (bone volume/total volume) in the micro-CT analysis was significantly higher in the defect filled with autograft and LF (100 $\mu\text{g/mL}$) group compared to that in the autograft only group. Thus, TA-MSN-LF conclusively induces bone tissue formation and spinal regeneration.

Park et al.³⁹ analyzed the effects of LF in a rat model of calvarial defects. Histological evaluation of the osteogenic effects of LF revealed reduced bone defects in the group injected with LF compared to those in the control group ($p < 0.05$). A group treated with LF exhibited higher serum OCN levels than the control group.¹¹ Guo et al.¹¹ examined osteoblast-like cell metabolic activity at 24 h, which increased in the group that consumed LF. In the present study, OCN was stained and quantified. OCN staining was good in the TA-MSN-LF high and low groups, and the OCN intensity was significantly higher than that in the other groups. Additionally, the mRNA expression levels of OCN and OPN were significantly higher in the TA-MSN-LF high and low groups than in the other groups ($p < 0.05$). As a biologically active molecule, LF promotes the proliferation and differentiation of various cells.³⁰ It also inhibits osteoclast formation by reducing the number of osteoclasts that can actively resorb bone.⁴¹ These positive effects of LF support its application in bone tissue regeneration. However, the low bioavailability of LF *in vivo* has facilitated the development of nanomaterial-based strategies to improve the biological activity of LF. This *in vitro* study demonstrated that TA-MSN-LF promotes osteogenesis and angiogenesis. Although the present study did not compare TA-MSN-LF with other materials, Chang et al. reported that 100 μg of LF produced more substantial osteoinductive effects than BMP-

2, concluding that LF could replace BMP-2.²⁷ Similarly, evaluation of the osteoblast differentiation ability of LF revealed that 100 μg was the most effective dose.²⁸ Furthermore, Zhang et al.²⁹ reported that 100 μg of LF was most effective in promoting the proliferative activity of osteoblast cells. Considering the importance of bone fusion ability, high-dose TA-MSN-LF (100 $\mu\text{g}/\text{mL}$) excellently induced differentiation and promoted proliferation in bone tissue engineering in the present study.

This study had several limitations. First, the sample size was small (eight rats in each group). However, this is the first experimental report confirming the effect of LF in a spinal fusion model. Second, because the effect of LF was evaluated at a single time point, the degree of healing could not be assessed in all groups over various periods. Third, only one graft material was used; we were unable to evaluate the effect of LF on bone healing using other graft materials (e.g., allografts). Nevertheless, to the best of our knowledge, this is the first study to demonstrate that LF induces effective bone fusion in a spinal fusion model. However, further studies are required to elucidate the systemic side effects and local complications and to establish safe and effective doses of LF. Moreover, clinical trials are required to demonstrate the clinical outcomes of LF.

V. CONCLUSION

TA-MSN-LF possessed effective bone fusion and angiogenesis effects in rats, which suggests that it is a potent material for spinal bone fusion. In particular, the bone fusion ability of high-concentration TA-MSN-LF (100 $\mu\text{g}/\text{mL}$) was higher than that of low-concentration TA-MSN-LF (1 $\mu\text{g}/\text{mL}$).

REFERENCES

1. Reid, J.J.; Johnson, J.S.; Wang, J.C. Challenges to Bone Formation in Spinal Fusion. *J. Biomech.* **2011**, *44*, 213-220.
2. Steinmann, J.C.; Herkowitz, H.N. Pseudarthrosis of the Spine. *Clin. Orthop. Relat. Res.* **1992**, *284*, 80-90.
3. Glassman SD, Polly DW, Bono CM, Burkus K, Dimar JR. Outcome of lumbar arthrodesis in patients sixty-five years of age or older. *J. Bone Joint Surg. Am.* **2009**, *91*(4), 783–90.
4. Patel, V.V.; Wuthrich, Z.R.; Ortega, A.; Ferguson, V.L.; Lindley, E.M. Recombinant Human Bone Morphogenetic Protein–2 Improves Spine Fusion in a Vitamin D–Deficient Rat Model. *Int. J Spine Surg.* **2020**, *14*, 694-705.
5. Benzel E, Ferrara L, Roy S, et al. Micromachines in spine surgery. *Spine* **2004**, *29*, 601–606.
6. Lee JY, Lim H, Ahn JW, et al. Design of a 3D BMP-2- delivering tannylated PCL scaffold and its anti-oxidant, anti-inflammatory, and osteogenic effects in vitro. *Int. J. Mol. Sci.* **2018**, *19*, 3602.
7. Hettiaratchi MH, Krishnan L, Rouse T, et al. Heparin-mediated delivery of bone morphogenetic protein-2 improves spatial localization of bone regeneration. *Sci Adv.* 2020 Jan 3;*6*(1):eaay1240.
8. Cornish, J.; Naot, D. Lactoferrin as an Effector Molecule in the Skeleton. *Biometals* **2010**, *23*, 425-430. [https://doi.org/ 10.1007/s10534-010-9320-6](https://doi.org/10.1007/s10534-010-9320-6). Epub 2010 Mar 16.
9. Brock, J.H. *The Physiology of Lactoferrin.* 2002.
10. Yanagisawa, S.; Nagasaki, K.; Chea, C.; Ando, T.; Ayuningtyas, N.F.; Inubushi, T.; Ishikado, A.; Imanaka, H.; Sugiyama, E.; Takahashi, I. *et al.* Oral Administration of Bovine Lactoferrin Suppresses the Progression of Rheumatoid Arthritis in an SKG Mouse Model. *PLoS ONE* **2022**, *17*.

11. Guo, H.Y.; Jiang, L.; Ibrahim, S.A.; Zhang, L.; Zhang, H.; Zhang, M.; Ren, F.Z. Orally Administered Lactoferrin Preserves Bone Mass and Microarchitecture in Ovariectomized Rats. *J. Nutr.* **2009**, *139*, 958-964.
12. Cornish J, Callon KE, Naot D, Palmano KP, Banovic T, Bava U, Watson M, Lin JM, Tong PC, et al. Lactoferrin is a potent regulator of bone cell activity and increases bone formation in vivo. *Endocrinology* **2004**, *145*, 4366-74.
13. 33. Sehrawat, A.; Sharma, S.; Sultana, S. Preventive effect of tannic acid on 2-acetylaminofluorene induced antioxidant level, tumor promotion and hepatotoxicity: A chemopreventive study. *Redox. Rep.* 2006, *11*, 85-95.
14. 34. Abouelmagd, S.A.; Meng, F.; Kim, B.K.; Hyun, H.; Yeo, Y. Tannic acid-mediated surface functionalization of polymeric nanoparticles. *ACS Biomater. Sci. Eng.* 2016, *2*, 2294-2303.
15. 35. Lee, J.Y.; Lim, H.; Ahn, J.W.; Jang, D.; Lee, S.H.; Park, K.; Kim, S.E. Design of a 3D BMP-2-Delivering Tannylated PCL Scaffold and Its Anti-Oxidant, Anti-Inflammatory, and Osteogenic Effects In Vitro. *Int. J. Mol. Sci.* 2018, *19*, 3602.
16. 36. Liang, H.; Zhou, B.; Wu, D.; Li, J.; Li, B. Supramolecular design and applications of polyphenol-based architecture: A review. *Adv. Colloid. Interface Sci.* 2019, *272*, 102019.
17. 37. Singh, N.; Karambelkar, A.; Gu, L.; Lin, K.; Miller, J.S.; Chen, C.S.; Sailor, M.J.; Bhatia, S.N. Bioresponsive mesoporous silica nanoparticles for triggered drug release. *J. Am. Chem. Soc.* 2011, *133*, 19582-19585.
18. 38. Chen, Z.; Li, X.; He, H.; Ren, Z.; Liu, Y.; Wang, J.; Li, Z.; Shen, G.; Han, G. Mesoporous silica nanoparticles with manipulated microstructures for drug delivery. *Colloids. Surf. B Biointerfaces* 2012, *95*, 274-278.
19. 39. Kuo, Y.C.; Wang, C.C. Surface modification with peptide for enhancing chondrocyte adhesion and cartilage regeneration in porous scaffolds. *Colloids. Surf. B Biointerfaces* 2011, *84*, 63-70.

20. 40. Watermann, A.; Brieger, J. Mesoporous Silica Nanoparticles as Drug Delivery Vehicles in Cancer. *Nanomaterials-Basel* 2017, 7, 189.
21. Noh, S.H.; Jo, H.; Choi, S.; Song, H.G.; Kim, H.; Kim, K.N.; Kim, S.E.; Park, K. Lactoferrin-Anchored Tannylated Mesoporous Silica Nanomaterials for Enhanced Osteo-Differentiation Ability. *Pharmaceutics* **2020**, 13, 30.
22. Choi, H.J.; Choi, S.; Kim, J.G.; Song, M.H.; Shim, K.S.; Lim, Y.M.; Kim, H.J.; Park, K.; Kim, S.E. Enhanced tendon restoration effects of anti-inflammatory, lactoferrin-immobilized, heparin-polymeric nanoparticles in an Achilles tendinitis rat model. *Carbohydr. Polym.* **2020**, 241, 116284.
23. Singh, N.; Karambelkar, A.; Gu, L.; Lin, K.; Miller, J.S.; Chen, C.S.; Sailor, M.J.; Bhatia, S.N. Bioresponsive mesoporous silica nanoparticles for triggered drug release. *J. Am. Chem. Soc.* **2011**, 133(49), 19582-5.
24. Kuo, Y.C.; Wang, C.C. Surface modification with peptide for enhancing chondrocyte adhesion and cartilage regeneration in porous scaffolds. *Colloids Surf. B. Biointerfaces.* **2011**, 84(1), 63-70.
25. Abouelmagd, S.A.; Meng, F.; Kim, B.K.; Hyun, H.; Yeo, Y. Tannic acid-mediated surface functionalization of polymeric nanoparticles. *ACS Biomater. Sci. Eng.* **2016**, 12, 2(12), 2294-2303.
26. Liang, H.; Zhou, B.; Wu, D.; Li, J.; Li, B. Supramolecular design and applications of polyphenol-based architecture: A review. *Adv Colloid Interface Sci.* **2019**, 272, 102019.
27. Chang, Y.; Ping, A.; Chang, C.; Betz, V.M.; Cai, L.; Ren, B. Lactoferrin Mediates Enhanced Osteogenesis of Adipose-Derived Stem Cells: Innovative Molecular and Cellular Therapy for Bone Repair. *Int. J. Mol. Sci.* **2023**, 24, 1749.
28. Li, Y.; Wang, J.; Ren, F.; Zhang, W.; Zhang, H.; Zhao, L.; Zhang, M.; Cui, W.; Wang, X.; Guo, H. Lactoferrin Promotes Osteogenesis through TGF- β Receptor II Binding in Osteoblasts and Activation of Canonical TGF- β Signaling in MC3T3-E1 Cells and C57BL/6J Mice. *J Nutr.* 2018 Aug 1;148(8):1285-1292.

29. Zhang, J.; Han, X.; Shan, Y.; Zhang, L.; Du, M.; Liu, M.; Yi, H.; Ma, Y. Effect of bovine lactoferrin and human lactoferrin on the proliferative activity of the osteoblast cell line MC3T3-E1 in vitro. *J Dairy Sci.* 2018 Mar;101(3):1827-1833.
30. Yagi, M.; Suzuki, N.; Takayama, T.; Arisue, M.; Kodama, T.; Yoda, Y.; Otsuka, K.; Ito, K. Effects of Lactoferrin on the Differentiation of Pluripotent Mesenchymal Cells. *Cell Biol. Int.* **2009**, 33, 283-289.
31. Balasubramanian, S.A.; Pye, D.C.; Willcox, M.D.P. Levels of Lactoferrin, Secretory IgA and Serum Albumin in the Tear Film of People with Keratoconus. *Exp. Eye Res.* **2012**, 96, 132-137.
32. Montagne, P.; Cuillière, M.L.; Molé, C.; Béné, M.C.; Faure, G. Changes in Lactoferrin and Lysozyme Levels in Human Milk During the First Twelve Weeks of Lactation. In *Advances in Experimental Medicine and Biology*. Springer US: Boston, MA, 2001; 501, pp. 241-247.
33. Xu, Y.; An, J.; Tabys, D.; Xie, Y.; Zhao, T.; Ren, H.; Liu, N. Effect of Lactoferrin on the Expression Profiles of Long Non-Coding RNA during Osteogenic Differentiation of Bone Marrow Mesenchymal Stem Cells. *Int. J. Mol. Sci.* **2019**, 20, 4834.
34. Kim, S.E.; Lee, D.; Yun, Y.; Shim, K.; Jeon, D.I.; Rhee, J.; Kim, H.; Park, K. Heparin-Immobilized Hydroxyapatite Nanoparticles as a Lactoferrin Delivery System for Improving Osteogenic Differentiation of Adipose-Derived Stem Cells. *BMM.* **2016**, 11, 025004.
35. Amirthalingam, S.; Lee, S.S.; Rajendran, A.K.; Kim, I.; Hwang, N.S.; Rangasamy, J. Addition of Lactoferrin and Substance P in a Chitin/PLGA-CaSO₄ Hydrogel for Regeneration of Calvarial Bone Defects. *Mater. Sci. Eng. C Mater. Biol. Appl.* **2021**, 126:112172.
36. Li, W.; Zhu, S.; Hu, J. Bone Regeneration is Promoted by Orally Administered Bovine Lactoferrin in a Rabbit Tibial Distraction Osteogenesis Model. *Clin. Orthop. Relat. Res.* **2015**, 473, 2383-2393.

37. Li, W.; Hu, J.; Ji, P.; Zhu, S.; Zhu, Y. Oral Administration of Bovine Lactoferrin Accelerates the Healing of Fracture in Ovariectomized Rats. *J. Bone Miner. Metab.* **2020**, *38*, 648-657.
38. McRae, J.M.; Kennedy, J.A. Wine and Grape Tannin Interactions with Salivary Proteins and their Impact on Astringency: A Review of Current Research. *Molecules* **2011**, *16*, 2348-2364.
39. Park, Y.E.; Chandramouli, K.; Watson, M.; Zhu, M.; Callon, K.E.; Tuari, D.; Abdeltawab, H.; Svirskis, D.; Musson, D.S.; Sharma, M. et al. Sustained Delivery of Lactoferrin using Poloxamer Gels for Local Bone Regeneration in a Rat Calvarial Defect Model. *Materials* **2021**, *15*.
40. Koca, C.G.; Yildirim, B.; Ozmen, O.; Dikilitas, A.; Cicek, M.F.; Simsek, A.T.; Gungor, M.A.; Tuncay, E. Effect of Single-Dose Locally Applied Lactoferrin on Autograft Healing in Peri-Implant Bone in Rat Models. *Injury* **2022**, *53*, 858-867.
41. Icriverzi, M.; Dinca, V.; Moisei, M.; Evans, R.W.; Trif, M.; Roseanu, A. Lactoferrin in Bone Tissue Regeneration. *Curr. Med. Chem.* **2020**, *27*, 838-853.

ABSTRACT(IN KOREAN)

락토페린 고정 탄닐화된 메조다공성 실리카 나노물질의
척추 유합 향상 검증
<지도교수 김 공 년>

연세대학교 대학원 의학과

노 성 현

락토페린(LF)은 소와 인간의 초유에서 발견되는 강력한 항바이러스제, 항염증제, 항균제로서 골형성 성장 인자로 작용합니다. 본 연구는 쥐 모델에서 LF가 뼈 유합 물질로 기능하는지 여부를 조사하는 것을 목표로 했습니다. 본 연구에서는 LF 고정 탄닐화 메조포러스 실리카 나노물질(TA-MSN-LF)을 생성하고 척추 유합 동물 모델에서 낮은(1 μ g) 및 높은(100 μ g) TA-MSN-LF 농도의 효과를 측정했습니다. 연구에서 쥐는 결함, MSN, TA-MSN-LF-낮음(1 μ g/ml) 및 TA-MSN-LF-높음(100 μ g/ml)의 4개 그룹으로 분류되었습니다. 수술 후 8주째에는 TA-MSN-LF 군에서 다른 군에 비해 방사선학적 융합이 더 많이 확인되었다. 헤마톡실린 및 에오신 염색은 TA-MSN-LF 그룹에서 새로운 뼈 유합이 유도되었음을 보여주었습니다. 또한, 면역조직화학법을 통해 뼈 형성의 지표인 오스테오칼신이 검출되었고, 그 강도는 TA-MSN-LF 군에서 유도되었다. TA-MSN-LF-High 그룹에서는 새로운 혈관의 형성이 유도되었습니다. 또한 TA-MSN-LF 군에서 혈청 오스테오칼신 수치와 오스테오칼신 및 오스테오키프의 mRNA 발현이 증가함을 확인했습니다. TA-MSN-LF는 쥐에서 효과적인 뼈 유합과 혈관 신생을 보여주었습니다. 우리는

TA-MSN-LF가 척추뼈 유합을 위한 강력한 재료임을 제안합니다.

핵심되는 말: 락토펜, 뼈 유합, 쥐, 척추, 나노입자

PUBLICATION LIST

1. Reid, J.J.; Johnson, J.S.; Wang, J.C. Challenges to Bone Formation in Spinal Fusion. *J. Biomech.* **2011**, 44, 213-220.
2. Steinmann, J.C.; Herkowitz, H.N. Pseudarthrosis of the Spine. *Clin. Orthop. Relat. Res.* **1992**, 284, 80-90.
3. Glassman SD, Polly DW, Bono CM, Burkus K, Dimar JR. Outcome of lumbar arthrodesis in patients sixty-five years of age or older. *J. Bone Joint Surg. Am.* **2009**, 91(4), 783–90.
4. Patel, V.V.; Wuthrich, Z.R.; Ortega, A.; Ferguson, V.L.; Lindley, E.M. Recombinant Human Bone Morphogenetic Protein–2 Improves Spine Fusion in a Vitamin D–Deficient Rat Model. *Int. J Spine Surg.* **2020**, 14, 694-705.
5. Benzel E, Ferrara L, Roy S, et al. Micromachines in spine surgery. *Spine* **2004**, 29, 601–606.
6. Lee JY, Lim H, Ahn JW, et al. Design of a 3D BMP-2- delivering tannylated PCL scaffold and its anti-oxidant, anti-inflammatory, and osteogenic effects in vitro. *Int. J. Mol. Sci.* **2018**, 19, 3602.
7. Hettiaratchi MH, Krishnan L, Rouse T, et al. Heparin-mediated delivery of bone morphogenetic protein-2 improves spatial localization of bone regeneration. *Sci Adv.* 2020 Jan 3;6(1):eaay1240.
8. Cornish, J.; Naot, D. Lactoferrin as an Effector Molecule in the Skeleton. *Biometals* **2010**, 23, 425-430. [https://doi.org/ 10.1007/s10534-010-9320-6](https://doi.org/10.1007/s10534-010-9320-6). Epub 2010 Mar 16.
9. Brock, J.H. *The Physiology of Lactoferrin.* 2002.
10. Yanagisawa, S.; Nagasaki, K.; Chea, C.; Ando, T.; Ayuningtyas, N.F.; Inubushi, T.; Ishikado, A.; Imanaka, H.; Sugiyama, E.; Takahashi, I. *et al.* Oral Administration of Bovine Lactoferrin Suppresses the Progression of Rheumatoid Arthritis in an SKG Mouse Model. *PLoS ONE* **2022**, 17.

11. Guo, H.Y.; Jiang, L.; Ibrahim, S.A.; Zhang, L.; Zhang, H.; Zhang, M.; Ren, F.Z. Orally Administered Lactoferrin Preserves Bone Mass and Microarchitecture in Ovariectomized Rats. *J. Nutr.* **2009**, *139*, 958-964.
12. Cornish J, Callon KE, Naot D, Palmano KP, Banovic T, Bava U, Watson M, Lin JM, Tong PC, et al. Lactoferrin is a potent regulator of bone cell activity and increases bone formation in vivo. *Endocrinology* **2004**, *145*, 4366-74.
13. 33. Sehrawat, A.; Sharma, S.; Sultana, S. Preventive effect of tannic acid on 2-acetylaminofluorene induced antioxidant level, tumor promotion and hepatotoxicity: A chemopreventive study. *Redox. Rep.* 2006, *11*, 85-95.
14. 34. Abouelmagd, S.A.; Meng, F.; Kim, B.K.; Hyun, H.; Yeo, Y. Tannic acid-mediated surface functionalization of polymeric nanoparticles. *ACS Biomater. Sci. Eng.* 2016, *2*, 2294-2303.
15. 35. Lee, J.Y.; Lim, H.; Ahn, J.W.; Jang, D.; Lee, S.H.; Park, K.; Kim, S.E. Design of a 3D BMP-2-Delivering Tannylated PCL Scaffold and Its Anti-Oxidant, Anti-Inflammatory, and Osteogenic Effects In Vitro. *Int. J. Mol. Sci.* 2018, *19*, 3602.
16. 36. Liang, H.; Zhou, B.; Wu, D.; Li, J.; Li, B. Supramolecular design and applications of polyphenol-based architecture: A review. *Adv. Colloid. Interface Sci.* 2019, *272*, 102019.
17. 37. Singh, N.; Karambelkar, A.; Gu, L.; Lin, K.; Miller, J.S.; Chen, C.S.; Sailor, M.J.; Bhatia, S.N. Bioresponsive mesoporous silica nanoparticles for triggered drug release. *J. Am. Chem. Soc.* 2011, *133*, 19582-19585.
18. 38. Chen, Z.; Li, X.; He, H.; Ren, Z.; Liu, Y.; Wang, J.; Li, Z.; Shen, G.; Han, G. Mesoporous silica nanoparticles with manipulated microstructures for drug delivery. *Colloids. Surf. B Biointerfaces* 2012, *95*, 274-278.
19. 39. Kuo, Y.C.; Wang, C.C. Surface modification with peptide for enhancing chondrocyte adhesion and cartilage regeneration in porous scaffolds. *Colloids. Surf. B Biointerfaces* 2011, *84*, 63-70.

20. 40. Watermann, A.; Brieger, J. Mesoporous Silica Nanoparticles as Drug Delivery Vehicles in Cancer. *Nanomaterials-Basel* 2017, 7, 189.
21. Noh, S.H.; Jo, H.; Choi, S.; Song, H.G.; Kim, H.; Kim, K.N.; Kim, S.E.; Park, K. Lactoferrin-Anchored Tannylated Mesoporous Silica Nanomaterials for Enhanced Osteo-Differentiation Ability. *Pharmaceutics* **2020**, 13, 30.
22. Choi, H.J.; Choi, S.; Kim, J.G.; Song, M.H.; Shim, K.S.; Lim, Y.M.; Kim, H.J.; Park, K.; Kim, S.E. Enhanced tendon restoration effects of anti-inflammatory, lactoferrin-immobilized, heparin-polymeric nanoparticles in an Achilles tendinitis rat model. *Carbohydr. Polym.* **2020**, 241, 116284.
23. Singh, N.; Karambelkar, A.; Gu, L.; Lin, K.; Miller, J.S.; Chen, C.S.; Sailor, M.J.; Bhatia, S.N. Bioresponsive mesoporous silica nanoparticles for triggered drug release. *J. Am. Chem. Soc.* **2011**, 133(49), 19582-5.
24. Kuo, Y.C.; Wang, C.C. Surface modification with peptide for enhancing chondrocyte adhesion and cartilage regeneration in porous scaffolds. *Colloids Surf. B. Biointerfaces.* **2011**, 84(1), 63-70.
25. Abouelmagd, S.A.; Meng, F.; Kim, B.K.; Hyun, H.; Yeo, Y. Tannic acid-mediated surface functionalization of polymeric nanoparticles. *ACS Biomater. Sci. Eng.* **2016**, 12, 2(12), 2294-2303.
26. Liang, H.; Zhou, B.; Wu, D.; Li, J.; Li, B. Supramolecular design and applications of polyphenol-based architecture: A review. *Adv Colloid Interface Sci.* **2019**, 272, 102019.
27. Chang, Y.; Ping, A.; Chang, C.; Betz, V.M.; Cai, L.; Ren, B. Lactoferrin Mediates Enhanced Osteogenesis of Adipose-Derived Stem Cells: Innovative Molecular and Cellular Therapy for Bone Repair. *Int. J. Mol. Sci.* **2023**, 24, 1749.
28. Li, Y.; Wang, J.; Ren, F.; Zhang, W.; Zhang, H.; Zhao, L.; Zhang, M.; Cui, W.; Wang, X.; Guo, H. Lactoferrin Promotes Osteogenesis through TGF- β Receptor II Binding in Osteoblasts and Activation of Canonical TGF- β Signaling in MC3T3-E1 Cells and C57BL/6J Mice. *J Nutr.* 2018 Aug 1;148(8):1285-1292.

29. Zhang, J.; Han, X.; Shan, Y.; Zhang, L.; Du, M.; Liu, M.; Yi, H.; Ma, Y. Effect of bovine lactoferrin and human lactoferrin on the proliferative activity of the osteoblast cell line MC3T3-E1 in vitro. *J Dairy Sci.* 2018 Mar;101(3):1827-1833.
30. Yagi, M.; Suzuki, N.; Takayama, T.; Arisue, M.; Kodama, T.; Yoda, Y.; Otsuka, K.; Ito, K. Effects of Lactoferrin on the Differentiation of Pluripotent Mesenchymal Cells. *Cell Biol. Int.* **2009**, 33, 283-289.
31. Balasubramanian, S.A.; Pye, D.C.; Willcox, M.D.P. Levels of Lactoferrin, Secretory IgA and Serum Albumin in the Tear Film of People with Keratoconus. *Exp. Eye Res.* **2012**, 96, 132-137.
32. Montagne, P.; Cuillière, M.L.; Molé, C.; Béné, M.C.; Faure, G. Changes in Lactoferrin and Lysozyme Levels in Human Milk During the First Twelve Weeks of Lactation. In *Advances in Experimental Medicine and Biology*. Springer US: Boston, MA, 2001; 501, pp. 241-247.
33. Xu, Y.; An, J.; Tabys, D.; Xie, Y.; Zhao, T.; Ren, H.; Liu, N. Effect of Lactoferrin on the Expression Profiles of Long Non-Coding RNA during Osteogenic Differentiation of Bone Marrow Mesenchymal Stem Cells. *Int. J. Mol. Sci.* **2019**, 20, 4834.
34. Kim, S.E.; Lee, D.; Yun, Y.; Shim, K.; Jeon, D.I.; Rhee, J.; Kim, H.; Park, K. Heparin-Immobilized Hydroxyapatite Nanoparticles as a Lactoferrin Delivery System for Improving Osteogenic Differentiation of Adipose-Derived Stem Cells. *BMM.* **2016**, 11, 025004.
35. Amirthalingam, S.; Lee, S.S.; Rajendran, A.K.; Kim, I.; Hwang, N.S.; Rangasamy, J. Addition of Lactoferrin and Substance P in a Chitin/PLGA-CaSO₄ Hydrogel for Regeneration of Calvarial Bone Defects. *Mater. Sci. Eng. C Mater. Biol. Appl.* **2021**, 126:112172.
36. Li, W.; Zhu, S.; Hu, J. Bone Regeneration is Promoted by Orally Administered Bovine Lactoferrin in a Rabbit Tibial Distraction Osteogenesis Model. *Clin. Orthop. Relat. Res.* **2015**, 473, 2383-2393.

37. Li, W.; Hu, J.; Ji, P.; Zhu, S.; Zhu, Y. Oral Administration of Bovine Lactoferrin Accelerates the Healing of Fracture in Ovariectomized Rats. *J. Bone Miner. Metab.* **2020**, *38*, 648-657.
38. McRae, J.M.; Kennedy, J.A. Wine and Grape Tannin Interactions with Salivary Proteins and their Impact on Astringency: A Review of Current Research. *Molecules* **2011**, *16*, 2348-2364.
39. Park, Y.E.; Chandramouli, K.; Watson, M.; Zhu, M.; Callon, K.E.; Tuari, D.; Abdeltawab, H.; Svirskis, D.; Musson, D.S.; Sharma, M. et al. Sustained Delivery of Lactoferrin using Poloxamer Gels for Local Bone Regeneration in a Rat Calvarial Defect Model. *Materials* **2021**, *15*.
40. Koca, C.G.; Yildirim, B.; Ozmen, O.; Dikilitas, A.; Cicek, M.F.; Simsek, A.T.; Gungor, M.A.; Tuncay, E. Effect of Single-Dose Locally Applied Lactoferrin on Autograft Healing in Peri-Implant Bone in Rat Models. *Injury* **2022**, *53*, 858-867.
41. Icriverzi, M.; Dinca, V.; Moisei, M.; Evans, R.W.; Trif, M.; Roseanu, A. Lactoferrin in Bone Tissue Regeneration. *Curr. Med. Chem.* **2020**, *27*, 838-853.